



Universiteit
Leiden
The Netherlands

Radio galaxies at low frequencies: high spatial and spectral resolution studies with LOFAR

Morabito, L.K.

Citation

Morabito, L. K. (2016, September 13). *Radio galaxies at low frequencies: high spatial and spectral resolution studies with LOFAR*. Retrieved from <https://hdl.handle.net/1887/43072>

Version: Not Applicable (or Unknown)

License:

Downloaded from: <https://hdl.handle.net/1887/43072>

Note: To cite this publication please use the final published version (if applicable).

Cover Page



Universiteit Leiden



The handle <http://hdl.handle.net/1887/43072> holds various files of this Leiden University dissertation.

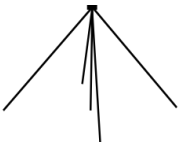
Author: Morabito, L.K.

Title: Radio galaxies at low frequencies: high spatial and spectral resolution studies with LOFAR

Issue Date: 2016-09-13

Radio Galaxies at Low Frequencies

high spatial and spectral resolution studies with LOFAR



Leah K. Morabito

© 2016 Leah K. Morabito

ISBN: 978-90-9029907-5

Cover: Design and images by Leah K. Morabito.

Background: A portion of a wide-field image around a high redshift radio galaxy, 4C 39.37, at 56MHz using only 2MHz of bandwidth from a Low Frequency Array observation made with the Low Band Antenna.

Foreground: At the top is a representation of a Low Band Antenna dipole. In the left circle is the stacked line profile from the first extragalactic detection of carbon radio recombination lines, and in the right circle are smoothed contours from the highest resolution image at frequencies below 100MHz.

Radio Galaxies at Low Frequencies

high spatial and spectral resolution studies with LOFAR

Proefschrift

ter verkrijging van
de graad van Doctor aan de Universiteit Leiden,
op gezag van Rector Magnificus prof. mr. C.J.J.M. Stolker,
volgens besluit van het College voor Promoties
te verdedigen op dinsdag 13 september 2016
klokke 13:45 uur

door

Leah K. Morabito

geboren te Englewood, Colorado, Verenigde Staten
in 1983

Promotiecommissie

Promotor: Prof. dr. Huub Röttgering Leiden University

Co-Promotor: Prof. dr. George Miley Leiden University

Overige leden:	Prof. dr. Michael Garrett	ASTRON/Leiden University
	Prof. dr. Raffaella Morganti	ASTRON/University of Groningen
	Prof. dr. Alexander Tielens	Leiden University
	Prof. dr. Huib van Langevelde	JIVE/Leiden University
	Dr. Adam Deller	ASTRON
	Dr. Huib Intema	Leiden University
	Dr. Raymond Oonk	ASTRON/Leiden University

*To follow knowledge like a sinking star,
Beyond the utmost bound of human thought.*
« Alfred Lord Tennyson »

Contents

1	Introduction	1
1.1	Early Radio Astronomy and Distant Radio Galaxies	1
1.2	High-Redshift Radio Galaxies	2
1.2.1	Characteristics	2
1.2.2	Feedback Processes	5
1.2.3	Open Questions	6
1.3	Active Galactic Nuclei	6
1.4	Low Frequency Carbon Radio Recombination Lines	9
1.4.1	The Cold Neutral Medium	9
1.4.2	Observing Carbon Radio Recombination Lines	10
1.4.3	Theoretical Models	10
1.5	Advances in Low Frequency Radio Astronomy	12
1.6	This Thesis	15
1.7	The Future is Bright at Low Frequencies	18
2	RGs and QSOs in Boötes	21
2.1	Introduction	22
2.2	The Boötes Field Data	24
2.2.1	AGES: Multi-wavelength Data	25
2.2.2	AGES/LOFAR sample completeness	25
2.2.3	LOFAR Boötes Survey	26
2.3	LOFAR Results	28
2.3.1	Flat vs. steep-spectrum Sources	28
2.3.2	Quasars vs. Radio Galaxies	29
2.4	Comparison with Previous Samples	29
2.4.1	3CRR Sample	29
2.4.2	Molonglo Radio Catalogue Sample	32

2.4.3	Results	32
2.5	Discussion	38
2.5.1	Orientation Interpretation	38
2.5.2	Evolutionary Interpretation	41
2.6	Conclusions	41
3	4C 43.15 at 55MHz	43
3.1	Introduction	44
3.2	Observations and pre-processing	47
3.2.1	Radio Observatory Processing	47
3.3	Data Calibration	48
3.3.1	Initial flagging and data selection	48
3.3.2	Removal of bright off-axis sources	51
3.3.3	LOFAR beam correction and conversion to circular polarization	51
3.3.4	Time-independent station scaling	52
3.3.5	Phase calibration for Dutch stations	53
3.3.6	Combining core stations	53
3.3.7	Calibrator residual phase, delay, and rate	54
3.3.8	Calibrator phase self-calibration	55
3.3.9	Setting the flux density scale	56
3.3.10	Target residual phase, delay, and rate	58
3.3.11	Astrometric Corrections	61
3.4	Results	61
3.4.1	Morphology	63
3.4.2	Spectral Index Properties	64
3.5	Discussion	69
3.5.1	Ages of the radio lobes	70
3.5.2	Environmental interaction	70
3.6	Conclusions and Outlook	73
4	Investigating the cause of the $\alpha - z$ relation	75
4.1	Introduction	76
4.2	Initial Sample	77
4.2.1	Archival Radio Spectral Energy Distributions	77
4.2.2	Constructing a High-redshift Sample	80
4.3	Modelling the Selection Effects	80
4.3.1	k -correction	80

4.3.2	Inverse Compton from CMB	82
4.3.3	Observational Biases	82
4.4	Results	82
4.5	Discussion and Conclusions	84
5	CRRLs in M82	85
5.1	Introduction	86
5.2	Observations and Data Reduction	87
5.3	Spectral Processing	89
5.3.1	Individual subband processing	89
5.3.2	Measuring the velocity/redshift	89
5.3.3	Reconstructing the Line Profile	92
5.4	Results	95
5.5	Discussion	95
5.6	Conclusions	96
6	Characterizing the CNM in M82	99
6.1	Introduction	100
6.2	Observations	101
6.3	Data Reduction	103
6.4	Extracting and Stacking the CRRLs	106
6.5	Results	108
6.6	Discussion	112
6.7	Conclusions	113
7	Gaunt Factors	115
7.1	Introduction	116
7.2	Oscillator Strength and the Gaunt Factor	117
7.3	Methods of Calculation	119
7.3.1	Asymptotic Expansion	119
7.3.2	Recursion Relations	120
7.3.3	OPACITY Project	121
7.4	Arbitrary-Precision Calculations	121
7.5	Comparison of Other Methods of Calculation	123
7.5.1	Comparison with Asymptotic Expansion	123
7.5.2	Relative Differences Between Methods	123
7.6	Conclusions	126

A Demixing LOFAR Long Baselines	129
A.1 Introduction	129
A.2 Data Reduction and Inspection	130
A.3 Demixing Simulation Input Models	131
A.4 Results	133
A.5 Conclusions	133
B The LOFAR Station Adder	135
B.1 Introduction	135
B.2 Diagnosing the Problem	135
B.3 Fixing the Problem	137
B.4 Conclusions	140
Bibliography	150
Samenvatting	151
English Summary	161
Publications	169
Curriculum Vitae	171
Acknowledgements	173

List of Figures

Chapter 1	1
1.1 Examples of Fanaroff-Riley FRI and FR II sources	3
1.2 The correlation between spectral index and redshift for bright radio galaxies	4
1.3 A diagram of a radio loud high-excitation AGN	8
1.4 LOFAR locations, the Chilbolton station, and LBA dipoles . . .	14
Chapter 2	21
2.1 Comparison of redshift and radio angular size for LOFAR-detected AGN in AGES	27
2.2 Cumulative linear sizes for flat-spectrum and steep-spectrum ra- dio sources	30
2.3 Cumulative linear sizes for radio galaxies and quasars	31
2.4 Power versus redshift for all samples	34
2.5 Linear sizes of radio galaxies and quasars versus redshift	36
2.6 Linear size ratio versus power and redshift	37
2.7 Quasar fraction versus linear size ratio	39
Chapter 3	43
3.1 Block diagram of calibration steps	50
3.2 Amplitude solutions for all stations	57
3.3 Spectral energy distribution of 3C 147	59
3.4 3C 147 imaged at 54MHz	60
3.5 Final LBA images of 4C 43.15 at 54MHz	62
3.6 Contours and intensity profiles for 4C 43.15 at four frequencies	65
3.7 The total integrated spectrum of 4C 43.15	66

3.8	Point-to-point spectral index values	68
3.9	The spatial distribution of the radio emission compared with H α line emission	72
Chapter 4		75
4.1	Distributions of initial spectral modelling parameters	79
4.2	$\alpha - z$ for the initial sample	80
4.3	k -corrected sample and distributions of redshifts	81
4.4	The $\alpha - z$ for the observed and simulated samples	83
Chapter 5		85
5.1	The spectral extraction process for M82	90
5.2	Cross-correlation between observed and model spectrum	91
5.3	Stacked CRRL spectrum	93
5.4	Smoothed CRRL spectrum	94
5.5	Comparison of CRRL spectrum with other gas tracers	97
Chapter 6		99
6.1	Stacked CRRL spectrum from spectral windows 1 and 2	107
6.2	Confidence intervals for CRRL optical depths for a grid of T_e and n_e	110
6.3	Integrated optical depths with best-fit models	111
Chapter 7		115
7.1	Gaunt factor values for transitions amongst levels up to $n = 2000$	124
7.2	Differences in values of the Gaunt factor calculated using the asymptotic expansion and the analytic expression	125
7.3	Comparison of different methods of calculating the Gaunt factor	127
Appendix A		129
A.1	A-team elevation	131
A.2	Visibility amplitudes versus time	132
A.3	Model of Cygnus-A like source	133
A.4	Simulation visibility amplitudes versus time	134

Appendix B	135
B.1 Comparison of images of 3C 147 before and after StationAdder	136
B.2 Differences in uncombined and combined visibilities	138
B.3 Comparison of before and after correct weight sum of visibilities with StationAdder	139

List of Tables

Chapter 1	1
1.1 General properties of different ISM components	11
Chapter 2	21
2.1 A summary of the different radio samples	33
Chapter 3	43
3.1 Observational summary	49
3.2 Summary of archival VLA data and re-imaging parameters . .	63
3.3 Integrated Flux Density Measurements.	67
3.4 Source parameters	69
Chapter 6	99
6.1 Observational summary of the data taken with the JVLA.	102
6.2 Details of spectral windows and flagging percentages	104
Chapter 7	115
7.1 A Sample of Methods of Calculating Oscillator Strength	122
Appendix A	129
A.1 Model parameters	132
Appendix B	135
B.1 IMFIT calculated noise	140

